

CHEM MED CHEM

CHEMISTRY ENABLING DRUG DISCOVERY

Accepted Article

Title: Carbon chain length modulates MDA-MB-231 breast cancer cell killing mechanisms by mitochondrially targeted aryl-urea fatty acids

Authors: Michael Murray, Ariane Roseblade, Yongjuan Chen, Kirsi Bourget, and Tristan Rawling

This manuscript has been accepted after peer review and appears as an Accepted Article online prior to editing, proofing, and formal publication of the final Version of Record (VoR). This work is currently citable by using the Digital Object Identifier (DOI) given below. The VoR will be published online in Early View as soon as possible and may be different to this Accepted Article as a result of editing. Readers should obtain the VoR from the journal website shown below when it is published to ensure accuracy of information. The authors are responsible for the content of this Accepted Article.

To be cited as: *ChemMedChem* 10.1002/cmdc.201900577

Link to VoR: <http://dx.doi.org/10.1002/cmdc.201900577>

WILEY-VCH

www.chemmedchem.org



Carbon chain length modulates MDA-MB-231 breast cancer cell killing mechanisms by mitochondrially targeted aryl-urea fatty acids

Prof. Michael Murray*^[a], Dr. Ariane Roseblade^[b], Dr. Yongjuan Chen^[a], Kirsi Bourget^[a] and Dr. Tristan Rawling^[b]

[a] Prof. M. Murray*, Dr. Y. Chen, K. Bourget
Discipline of Pharmacology, School of Medical Sciences, Faculty of Medicine and Health
University of Sydney
Camperdown, New South Wales, 2006, AUSTRALIA
*E-mail: michael.murray@sydney.edu.au

[b] Dr. A. Roseblade, Dr. T. Rawling
School of Mathematical and Physical Sciences, Faculty of Science
University of Technology Sydney
Ultimo, New South Wales, 2007, AUSTRALIA

Supporting information for this article is given via a link at the end of the document

Abstract: Targeting the tumor cell mitochondrion could produce novel anti-cancer agents. We designed an aryl-urea fatty acid (**1g**; 16({[4-chloro-3-(trifluoromethyl)phenyl]carbamoyl}amino)hexadecanoic acid) that disrupted the mitochondrion and decreased MDA-MB-231 breast cancer cell viability. To optimize the aryl-ureas the present study evaluated mitochondrial targeting by **1g** analogues containing alkyl chains between 10-17 carbons. Using the dye JC-1, the C12-C17 analogues efficiently disrupted the mitochondrial membrane potential (IC₅₀s 3.5±1.2 to 7.6±1.1 μM) and impaired ATP production; shorter analogues were less active. 7-Aminoactinomycin D/annexin V staining and flow cytometry showed that these agents activated the killing mechanisms of necrosis and apoptosis to varying extents (7-aminoactinomycin D/annexin V staining ratios 4.3-6.0). Indeed, **1g** and its C17 analogue preferentially activated necrosis and apoptosis, respectively (ratios 2.1 and 16). Taken together, alkyl chain length is a determinant of mitochondrial targeting by aryl-ureas and can be varied to develop analogues that activate apoptosis or necrosis in a regulated fashion.

Introduction

Molecules that kill cancer cells by novel mechanisms could lead to the development of new anti-cancer agents and agents that enable drug resistance to be overcome when used in combination with conventional oncology drugs. The mitochondrion controls energy metabolism and cell proliferation, as well as cell death and survival.^[1] These mechanisms are regulated differently in tumor cells, which creates the opportunity for the development of new anticancer agents that selectively target cancer cell mitochondria to induce cell death.

ω-3 Polyunsaturated fatty acids (ω-3 PUFAs), such as eicosapentaenoic acid (ω-3 C20:5), decrease tumorigenesis while the corresponding ω-6 PUFA, like arachidonic acid, promote tumour development.^[2-4] Thus, ω-3 PUFA could be utilized in novel anti-cancer drug development programs. In cells PUFA undergo biotransformation to diverse lipid mediators, including prostaglandins, leukotrienes and epoxides, that

modulate homeostasis.^[5] Cytochromes P450 (CYPs) have been studied extensively for their roles in the oxidative biotransformation of drugs and diverse foreign compounds,^[6-9] but CYPs are also active in endobiotic metabolism, including PUFA epoxidation. Epoxyeicosatrienoic acids are produced by the actions of CYPs on the ω-6 PUFA arachidonic acid and have been shown to promote proliferation and protect cells against deleterious stimuli;^[10] in contrast, certain ω-3 PUFA epoxides are anti-proliferative.^[11,12] Thus, we found that the CYP-derived ω-3-17,18-epoxide of eicosapentaenoic acid and its fully-saturated synthetic analogue ω-3-17,18-epoxyeicosanoic acid impaired the viability of breast cancer cells by decreasing proliferation and activating apoptosis.^[11,13] Epoxides of ω-3 docosahexaenoic acid (22:6) are also reported to prevent tumor progression.^[12]

ω-3 Fatty acid epoxides are active *in vivo* provided they are coadministered with a soluble epoxide hydrolase inhibitor to protect the labile epoxide group from enzymic hydration and degradation.^[14,15] Alternately, bioisosteric replacement of the epoxide moiety with urea has been used to generate epoxide mimetics that retain biological activity in the absence of soluble epoxide hydrolase inhibitors.^[16,17] Thus, we recently reported the development of an aryl-urea mimetic of ω-3-17,18-epoxyeicosanoic acid, termed **1g** (Figure 1, n=9), that targeted the mitochondrion and decreased the viability of MDA-MB-231 breast cancer cells *in vitro*, and inhibited tumour growth *in vivo* in mice carrying MDA-MB-231 cell xenografts.^[18]

1g is a promising new lead compound for anti-cancer drug development, but its optimisation requires information on the structural requirements for activity. Structure-activity relationship studies have identified two pharmacophoric groups in the drug scaffold: the aryl system substituted with strongly electron-withdrawing substituents,^[18,19] and the carboxylate group that can be replaced with bioisosteric hydroxamic acid, oxo-thiadiazole or sulfonate moieties.^[20] In **1g** these two pharmacophores are linked together by a saturated 16 carbon alkyl chain. In the present study we explored a chain extension/contraction strategy to identify the optimal chain length for antiproliferative activity. A series of **1g** analogues with 10 (**1a**) to 17 (**1h**) carbon alkyl chains between the aryl urea and

carboxylate groups were prepared (Figure 1), and their activity was assessed in human MDA-MB-231 cells. The principal findings to emerge were that analogues of intermediate and longer chain length (C12-C17) effectively disrupted the mitochondrial membrane potential, impaired ATP production and promoted cell death.

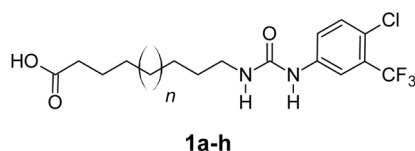


Figure 1. Chemical structures of lead aryl-urea substituted fatty acid **1g** ($n=9$) and analogues of varying alkyl chain length.

Results

Synthesis of aryl-urea analogues with altered alkyl chain length

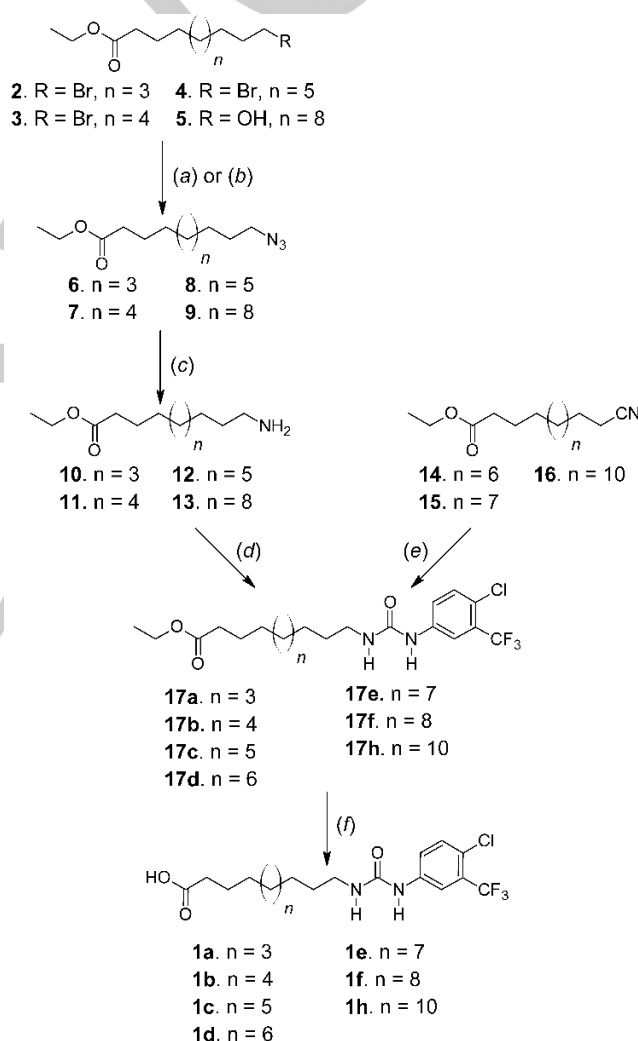
The synthesis of **1g** was reported previously.^[18] The procedure used to prepare the chain extension/contraction series was dependent on the commercial availability of starting materials (Scheme 1). Syntheses of analogues with 10, 11 and 12 carbon chains (**1a**, **1b** and **1c**, respectively) commenced from commercially available bromo-fatty acids, which had been ethyl ester-protected (**2-4**).^[21] In the first step **2-4** were reacted with NaN_3 to generate azides **6-8**. Staudinger reduction of the azides with triphenylphosphine and water yielded amines **10-12**, which were reacted with 4-chloro-3-(trifluoromethyl)phenyl isocyanate to generate ureas **17a – 17c**. Removal of the ester protecting groups with NaOH gave **1a**, **1b** and **1c**. The 15-carbon analogue **1f** was prepared similarly from the ester-protected hydroxy-fatty acid **5**, which was converted to azide **9** under Mitsunobu conditions.^[22]

Due to the limited commercial availability of appropriate hydroxy- or bromo-fatty acids **1d**, **1e** and **1h** were prepared by an alternate route that commenced from the nitriles **14-16**. We previously reported the synthesis of **14-16** by alkyl-alkyl Negishi cross-coupling reactions catalyzed by the N-heterocyclic carbene [1,3-bis(2,6-diisopropylphenyl)imidazol-2-ylidene][3-chloropyridyl]palladium(II) dichloride.^[21] Reduction of the nitrile groups using nickel boride, which was generated *in situ* using sodium borohydride and a catalytic amount of nickel(II) chloride,^[21] produced crude amines that were immediately reacted with 4-chloro-3-(trifluoromethyl)phenyl isocyanate to give **17d**, **17e** and **17h**. Subsequent hydrolysis of the ester protecting groups gave **1d**, **1e** and **1h**.

Alkyl chain length in aryl urea fatty acids influences mitochondrial targeting in MDA-MB-231 cells

Using the membrane-permeable redox-active cationic dye JC-1 the aryl-urea **1g** has been found previously to target the mitochondrion in MDA-MB-231 cells.^[18] In the electronegative environment of the intact inner mitochondrial membrane JC-1 forms aggregates that fluoresce red. In cells containing damaged mitochondria that have lost their membrane potential,

JC-1 remains in its monomeric form and fluoresces green. We assessed the capacity of alkyl chain length-modified aryl-ureas based on **1g** to disrupt the mitochondrial membrane potential in MDA-MB-231 cells using JC-1 staining. Treatment of cells with **1g** analogues of differing chain length (**1h**) decreased the JC-1 red:green fluorescence ratio in cells, consistent with membrane depolarisation. Efficient mitochondrial disruption was produced by the analogues **1c** to **1h** (IC_{50} range $3.5 \pm 1.2 \mu\text{M}$ to $7.6 \pm 1.1 \mu\text{M}$; Figure 2) whereas the analogues with the shortest alkyl chains (**1a** and **1b**) were much less effective (IC_{50} s 99 ± 1 and $113 \pm 1 \mu\text{M}$, respectively). In accord with these findings, fluorescence spectroscopy showed that treatment ($10 \mu\text{M}$, 4 h) of MDA-MB-231 cells with all analogues, especially **1c** to **1h**, decreased the red fluorescence intensity and increased green fluorescence intensity (Figure 3; Figure S1).



Scheme 1. Synthesis of **1g** analogues in which the alkyl chain length was varied. Reagents and conditions: (a) NaN_3 , DMSO, rt, 18 h; (b) PPh_3 , diisopropyl azodicarboxylate, 0°C – rt, 30 min, diphenyl phosphoryl azide, rt, 4.5 h; (c) PPh_3 , rt, 8 h, then H_2O , rt, 16 h; (d) 4-chloro-3-(trifluoromethyl)phenyl isocyanate, anhydrous THF, rt, 2 h; (e) $\text{NiCl}_2 \cdot 6\text{H}_2\text{O}$, NaBH_4 , 0°C – rt, 2 h, and then 4-chloro-3-(trifluoromethyl)phenyl isocyanate; (f) 1.5M NaOH , ethanol/water, rt, 4 h.

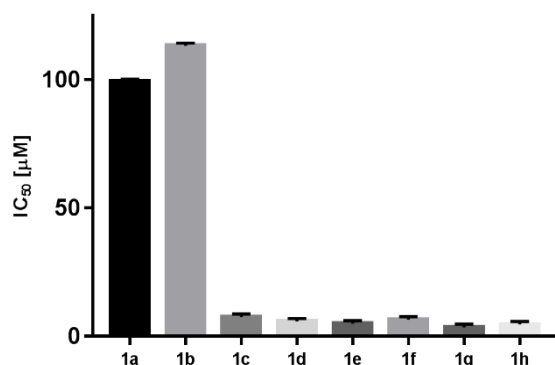


Figure 2. Mitochondrial targeting (JC-1 IC₅₀) by **1g** analogues of varying alkyl chain length. Data are means±SD obtained using 6-7 individual concentrations in at least triplicate experiments

Impaired ATP production by **1g** analogues in breast cancer cells

The impact of alkyl chain length-modified aryl-ureas on the viability of MDA-MB-231 cells was assessed using a series of approaches. ATP production was impaired significantly by all analogues (10 µM, 48 h), with the exception of **1a** (Figure 4A). Decreases were most pronounced for **1d**, **1f** and **1g** to 25±2%, 40±11% and 39±5% of control (P<0.001). In the control breast cell line MCF10A **1g** did not impair ATP production or cell viability.^[18]

Because ATP is required for cell proliferation we next used flow cytometry to evaluate the impact of the alkyl chain-modified aryl-ureas on cell cycle kinetics. Significant decreases in the population of cells in G₀G₁ phase, which reflects the proportion of cycling cells, were produced by analogues with alkyl chains of at least 13 carbons (range 54-67% versus 76% in control; Table 1; Figure 4B, Figure S2). All analogues, especially **1b** and longer, decreased the proportion of cells in G₂M phase (4.4-6.8% versus 9.3% in control; Table 1, P<0.001). In addition, analogues **1c-1e** containing alkyl chains of 12-14 carbons in length increased the proportion of cells accumulating in S-phase (9.6-11.4% versus 6.5% in control; Table 1, P<0.001). This suggests that analogues with alkyl chains greater than 11 carbons decrease cell viability in part by preventing completion of the cell cycle and impairing mitosis.

Flow cytometry also provides an estimate of cells with low DNA content (subG₁ phase). As shown in Table 1, marked increases in subG₁ phase were effected by treatment with analogues containing alkyl chains of 15-17 carbons (~5-fold of control; P<0.001), while less pronounced increases were produced by the C13 and C14 analogues to ~2-3-fold of control (P<0.001 and P<0.01, respectively).

Activation of cell killing by chain length-modified aryl-ureas

The increase in subG₁ phase suggests that longer chain analogues promote cell killing, which depletes DNA content. Mechanisms of cell killing were further assessed using staining with annexin V-FITC/7-aminoactinomycin D (7AAD) in cells that had been treated with **1a** to **1h** for 24 or 48 h. Decreases in the unstained (live) cell population were noted after 24 h treatment

with analogues from **1b** to **1h** (58.3-71.6% of total cells versus 80.7±0.3% of total in DMSO-treated control cells; Figure 5A, Figure S3; Table 2); similar findings were produced by 48 h of treatment (Table S1). In accord with these findings the active analogues increased both 7AAD and annexin V staining, consistent with increases in early necrosis and apoptosis, respectively, but to varying extents (Table 2). The most pronounced increase in 7AAD-stained cells to ~5-fold of control was effected by **1g** itself, with lesser increases by **1b**, **1c** and **1f** and trends toward an increase in staining produced by other analogues (Table 2).

In contrast with these findings, **1h** did not increase 7AAD staining over control. Instead, this analogue produced a strong increase in annexin V staining to ~2.4-fold of control at 24 h (22.6±2.6% versus 9.5±0.5% in control; Table 2, P<0.001); smaller increases in annexin V staining were effected by shorter chain analogues. Increased dual staining by annexin V/7AAD, reflecting late necrosis and apoptosis, was produced by most analogues after 24 h of treatment. These findings suggest that the balance between the death mechanisms of apoptosis and necrosis in **1g** analogues varies according to alkyl chain length (Figure 5B). Thus, although the shortest analogue (**1a**) had relatively low activity, **1b** to **1f** activated both necrosis and apoptosis, resulting in annexin V/7AAD staining ratios in the range 4.3-6.0 at 24 h, relative to control (ratio 6.5; Table 2); similar ratios were produced by 48 h of treatment (Table S1).

There was a noticeable difference in the apparent killing modes of the two longest chain analogues from a pronounced activation of necrosis for **1g**, as evidenced by strong 7AAD staining and a smaller increase in annexin V staining, to predominantly apoptosis for **1h** (strong annexin V and dual staining, with no increase staining by 7AAD over control). This is shown by the annexin V/7AAD staining ratios at 24 h of 2.1 and 16 for **1g** and **1h**, respectively (Table 2, Figure 5B); similar ratios were noted after 48 h of treatment (Table S1).

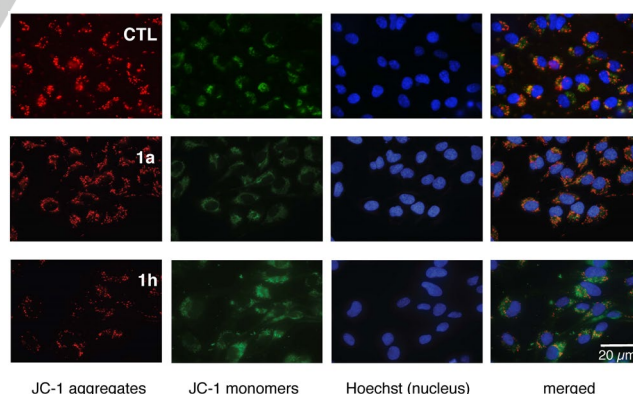


Figure 3. Fluorescence microscopy of MDA-MB-231 cells after treatment with analogues **1a** and **1h** (C10 and C17 chains; 10 µM, 4 h) or DMSO (CTL) 16 h after serum deprivation. After consecutive washes with serum-free medium, cells were incubated with JC-1 and Hoechst 33258 (Hoechst) for 20 min, according to the manufacturer's instructions. Fluorescence images of JC-1 aggregates (red), JC-1 monomers (green) and nucleus staining (blue) on cells were acquired with a fluorescence microscope (Olympus BX51, Notting Hill, VIC, Australia). Images for analogues **1b-1g** are shown in Fig S1

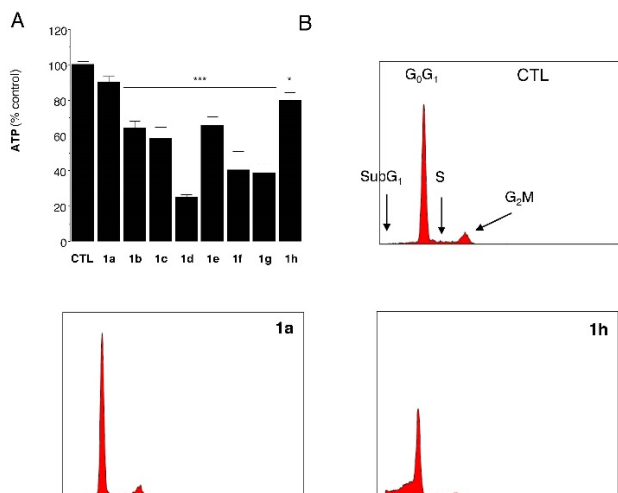


Figure 4. (A) Effects of aryl-ureas **1a** to **1h** (10 μ M, 48 h) on ATP formation by MDA-MB-231 cells. Basal ATP formation was 0.63 ± 0.02 nmol/ 7×10^4 MDA-MB-231 cells/24 h. (B) Flow cytometric analysis of control (CTL) MDA-MB-231 cells and cells after treatment with aryl-ureas **1a** and **1h** (10 μ M) for 48 h, showing the decrease in G₀G₁ and increases in S and subG₁ phases. All data are mean \pm SEM from three separate experiments. Different from DMSO-treated control: * $P < 0.05$, ** $P < 0.01$, *** $P < 0.001$. Histograms from cells treated with **1b-1g** are shown in Fig S2

Table 1. Alkyl chain length in **1g** analogues modulates cell cycle kinetics in MDA-MB-231 cells (48 h; 10 μ M)

Analogue	% cells			
	subG ₁	G ₀ G ₁	S	G ₂ M
control	5.97 \pm 0.49	75.7 \pm 1.0	6.50 \pm 0.40	9.27 \pm 0.62
1a	4.20 \pm 0.55	80.0 \pm 2.2	5.47 \pm 0.33	7.40 \pm 0.49**
1b	7.37 \pm 1.03	76.3 \pm 2.1	7.23 \pm 1.19	6.47 \pm 0.38***
1c	9.50 \pm 2.68	74.2 \pm 3.0	9.60 \pm 0.86**	5.53 \pm 0.33***
1d	20.63 \pm 2.24***	60.6 \pm 2.1***	11.37 \pm 0.44***	6.78 \pm 0.20***
1e	15.10 \pm 1.04*	67.2 \pm 1.2*	10.13 \pm 0.73**	5.90 \pm 0.32***
1f	30.63 \pm 4.49***	54.1 \pm 3.4***	8.50 \pm 0.79	5.30 \pm 0.70***
1g	25.37 \pm 4.17***	59.6 \pm 3.3***	7.10 \pm 0.81	5.57 \pm 0.17***
1h	31.73 \pm 2.71***	55.2 \pm 2.6***	6.23 \pm 0.75	4.37 \pm 0.33***

Different from control: * $P < 0.05$, ** $P < 0.01$, *** $P < 0.001$

Discussion

The development of well-tolerated oncology agents with novel mechanisms of action could provide therapeutic alternatives for the treatment of cancer patients. The long-chain fatty acid aryl-urea **1g** was recently identified as the prototype of a new class of agents that decrease the viability of MDA-MB-231 breast cancer cells by mitochondrial targeting.^[18] There are potential novel drug targets in the cancer cell mitochondrion due to structural and functional differences in the organelle from normal cells.^[1] Whereas oxidative phosphorylation is the primary

pathway for ATP synthesis in normal cells, aerobic glycolysis can predominate in aggressive tumor cells (the Warburg effect).^[23] Instead, the cancer cell mitochondrion is adapted for the increased production of macromolecules that are necessary for tumor cell replication.^[1] The mitochondrion also has an important role in cell death and survival; these pathways are frequently over-active in cancer cells so that the cell killing capacity of cytotoxic drugs is attenuated. New agents like **1g**, that selectively disrupt the mitochondrion in tumor cells, while leaving normal cell mitochondria undamaged, could target dysregulated mechanisms in tumor cells and lead to new therapeutic strategies.^[1,2,23]

Through structure-activity relationship studies we have identified two pharmacophoric groups in the aryl-urea fatty acid drug scaffold. Effective agents contained a terminal aryl system with strongly electron-withdrawing substituents.^[18,19] In addition, the carboxylate functionality is required for activity and can be replaced with bioisosteric hydroxamic acid, sulfonic acid or oxathiazole groups, but not by non-bioisosteric amide or ester functionalities.^[20] The present study evaluated the importance of the alkyl chain length in the activity of **1g** by preparing and testing analogues with chains that varied from 10 to 17 carbons. All of these aryl-urea fatty acid analogues disrupted the mitochondrial membrane potential, as reflected by the shift in the red:green fluorescence ratio with the dye JC-1. While the shortest chain analogues (**1a** and **1b**) were relatively non-potent (IC₅₀ ~100 μ M), the intermediate and longer chain analogues (**1c** to **1h**) were much more effective (IC₅₀s 3.5-7.6 μ M). It has been shown previously that other naturally occurring and synthetic saturated and unsaturated lipids can penetrate the mitochondrial membrane.^[24] For example, α -eleostearic acid produced a loss of mitochondrial membrane potential and activated mitochondrial apoptosis in MDA-MB-231 breast cancer cells.^[25] However, to our knowledge, the present study is the first to formally relate mitochondrial disruption to fatty acid structure in an homologous series of lipid analogues.

The present aryl-urea fatty acids, especially **1d**, **1f** and **1g**, decreased cellular ATP production and arrested cell cycle progression, which led to accumulation of cells in S phase and the failure to complete mitosis. Longer chain analogues also activated cell death mediated by the dual mechanisms of apoptosis and necrosis, as reflected by increases in the proportion of cells in subG₁ phase and annexin V/7AAD staining. Annexin V detects phosphatidylserine residues in the plasma membrane that are externalized during apoptosis, while disruption of the plasma membrane activates necrosis and enables DNA staining by 7AAD. The annexin V/7AAD staining ratio was used to quantify the relative importance of apoptosis and necrosis. Analogues **1a** to **1f** produced ratios that were similar to control, suggesting that both cell death pathways were increased to similar extents. Interestingly, however, the ratios produced by **1g** and **1h** were quite different (respectively 2.1 and 16 at 24 h, and 2.5 and 14 at 48 h) and are consistent with pronounced activation of necrosis and apoptosis, respectively. Taken together, these findings indicate that alkyl chain length can be modified to optimise the anti-proliferative and cell killing activities of **1g** analogues in MDA-MB-231 breast cancer cells. Our ongoing studies to identify the cellular target(s) of aryl-urea fatty acids may eventually provide additional mechanistic information to expand on the present findings.

It has been suggested that fatty acids may be useful adjunct agents to augment the activity of chemotherapeutic drugs. Previously we prepared a series of ω -3 monounsaturated fatty acids of chain length C16-C22 that decreased proliferation and increased apoptosis in MDA-MB-468 breast cancer cells that overexpressed the enzyme cyclooxygenase-2 (COX-2).^[21] In COX-2-dependent breast and colorectal cancers the administration of non-steroidal anti-inflammatory agents that inhibit COX-2 activity has been found to be an effective treatment, but toxicity has precluded their long-term use.^[26,27] An alternate approach could be co-treatment with anti-cancer lipids, such as the ω -3 monounsaturated fatty acids, that may be better tolerated. In designing such combination approaches the carbon

chain length in the lipid agent could be an important consideration.^[28]

The present findings suggest that chain length in aryl-ureas determines not only the efficacy of mitochondrial targeting but also the cell death mechanisms that are activated. Many investigations have focused on apoptosis as a major mechanism of tumor cell killing by oncology agents. More recently it has emerged that other forms of cell death, such as necrosis, are also activated by many established anti-cancer agents. Necrosis is activated by anthraquinones such as doxorubicin, as well as other cytotoxic agents like mitoxantrone, cisplatin and melphalan.^[29-31] Necrotic cells are characterized by mitochondrial swelling and loss of plasma membrane integrity without nuclear damage.^[32] Recently, Shen *et al.* screened ~1400 compounds to identify their mode of cell killing, with many agents activating either apoptosis or necrosis or both.^[33] A number of fatty acids and fatty acid metabolites were evaluated but the relationship between lipid structure and the mode of cell killing remained unclear. The findings in the present study suggest that the balance between the death mechanisms of apoptosis and necrosis in aryl-urea analogues varies according to chain length. Together, the present study with aryl-ureas suggests that it may now be feasible to utilise aryl-ureas to preferentially activate alternate death mechanisms in order to optimise tumour cell killing.

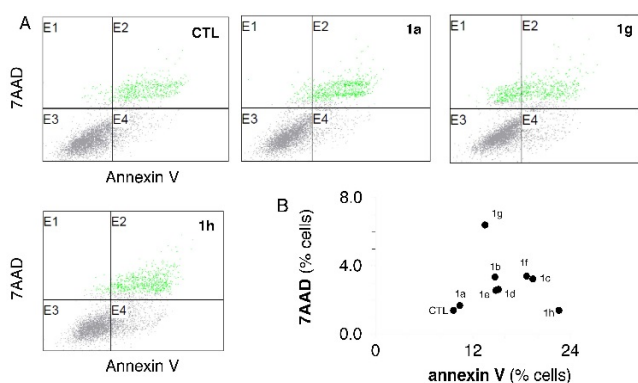


Figure 5. (A) Annexin V-FITC/7AAD staining in control (CTL) MDA-MB-231 cells after treatment with **1a**, **1g** and **1h** (10 μ M) for 24 h. 7AAD-stained cells (quadrant E1), annexin V-stained cells (quadrant E4), dual 7AAD and annexin V-stained cells (quadrant E3) and unstained live cells (quadrant E2) are shown. (B) Relationship between 7AAD stained and annexin V stained MDA-MB-231 cells by the aryl-ureas **1a** to **1h** (10 μ M) for 24 h. Data were derived in three separate experiments and representative images are shown. Cell staining after treatment with **1b-1f** are shown in Fig S3

Table 2. Alkyl chain length in **1g** analogues modulates cell cycle kinetics in MDA-MB-231 cells (48 h; 10 μ M)[†]

Analogue	7AAD	dual	live	annexin V	ratio
control	1.43 \pm 0.09	8.7 \pm 0.6	80.7 \pm 0.3	9.5 \pm 0.5	6.50
1a	1.73 \pm 0.37	15.2 \pm 0.7**	72.7 \pm 2.4	10.3 \pm 2.3	5.95
1b	3.40 \pm 0.50**	17.8 \pm 1.76***	64.2 \pm 1.6**	14.7 \pm 0.8	4.33
1c	3.27 \pm 0.33**	14.3 \pm 1.11***	63.2 \pm 1.2***	19.3 \pm 2.2**	5.90
1d	2.67 \pm 0.49	10.9 \pm 0.03	71.6 \pm 2.4*	15.1 \pm 2.9	5.66
1e	2.60 \pm 0.49	12.0 \pm 1.16	70.8 \pm 1.5*	14.8 \pm 2.2	5.69
1f	3.43 \pm 0.67**	14.0 \pm 1.21**	64.0 \pm 3.4**	18.5 \pm 2.8**	5.39
1g	6.47 \pm 0.37***	13.9 \pm 1.83**	70.4 \pm 6.3*	13.4 \pm 0.7	2.07
1h	1.43 \pm 0.09	18.0 \pm 1.42***	58.3 \pm 4.3***	22.6 \pm 2.6***	15.80

Different from control: *P<0.05, **P<0.01, ***P<0.001

[†]7AAD, % cells stained by 7-aminoactinomycin D; dual, % cells stained by both 7-aminoactinomycin D and annexin V; live, % unstained cells; annexin V, % cells stained by annexin V; ratio, ratio of cells stained by 7-aminoactinomycin D to cells stained by annexin V

Conclusion

In summary, we have prepared analogues of the novel anti-cancer aryl-urea **1g** in which the alkyl chain length was modified. Analogues containing longer alkyl chains promoted cell killing and decreased energy metabolism, whereas those with shorter alkyl chains were less active. It also emerged that the longest chain analogues - **1g** and **1h** - were not only effective in mitochondrial targeting but also preferentially activated the cell death mechanisms of necrosis and apoptosis, respectively. These agents may prove useful in unravelling the relationships between fatty acid chain length and selectivity in cell killing mechanisms in aryl-ureas.

Experimental Section

Chemistry

General: **1g**^[18], ester **5**^[22], nitrile **14**^[34] and compounds **2**, **3**, **4**, **15** and **16**^[21] were prepared as previously reported. All other reagents and anhydrous solvents were purchased from Sigma Aldrich (Castle Hill, NSW, Australia). Dry Column Vacuum Chromatography was used to purify reaction products on silica gel with gradient elutions. TLC was performed on silica gel 60 F₂₅₄ plates. Melting points were measured on a Stuart SMP10 melting point apparatus. ¹H and ¹³C NMR spectra were recorded on either a Varian 400-MR instrument or Agilent 500 MHz NMR. Spectra were referenced internally to residual solvent (CDCl₃; ¹H δ 7.26, ¹³C δ 77.10. *d*₆-DMSO; ¹H δ 2.49, ¹³C δ 39.52). High resolution mass spectrometry (HRMS) was performed on an Agilent Technologies 6510 Q-TOF LCMS.

General procedure for synthesis of azides from bromo esters

To a solution of the bromo ester (**2-4**, 20 mmol) in DMSO (75 mL) was added sodium azide (60 mmol). The resulting suspension was stirred at room temperature for 18 h. Ethyl acetate (250 mL) was added, and the resulting mixture was extracted with water (3 x 350 mL). The organic layer was dried and concentrated under reduced pressure to yield the desired products as oils.

Ethyl 10-azidodecanoate (6). Pale yellow oil, 94% yield. ¹H NMR (500 MHz, CDCl₃): δ 4.12 (q, *J* = 7.0 Hz, 2H), 3.25 (t, *J* = 7.0 Hz, 2H), 2.28 (t, *J* = 7.5 Hz, 2H), 1.50 – 1.65 (m, 4H), 1.20 – 1.40 (m, 13H). ¹³C NMR (125 MHz, CDCl₃): δ 173.88, 60.15, 51.44, 34.33, 29.32, 29.11, 29.05, 29.04, 28.79, 26.65, 24.91, 14.23. HRMS (ESI) *m/z* [M+H]⁺ calcd for C₁₂H₂₄N₃O₂, 242.1863; found, 242.1866.

Ethyl 11-azidoundecanoate (7). Pale yellow oil, 93% yield. ¹H NMR (500 MHz, CDCl₃): δ 4.11 (q, *J* = 7.0 Hz, 2H), 3.25 (t, *J* = 7.5 Hz, 2H), 2.28 (t, *J* = 7.5 Hz, 2H), 1.55 – 1.65 (m, 4H), 1.20 – 1.40 (m, 15H). ¹³C NMR (125 MHz, CDCl₃): δ 173.89, 60.14, 51.45, 34.35, 29.36, 29.78, 29.17, 29.08 (2C), 28.80, 26.66, 24.93, 14.23. HRMS (ESI) *m/z* [M+H]⁺ calcd for C₁₃H₂₆N₃O₂, 256.2020; found, 256.2019.

Ethyl 12-azidododecanoate (8). Pale yellow oil, 86% yield. ¹H NMR (500 MHz, CDCl₃): δ 4.12 (q, *J* = 7.0 Hz, 2H), 3.24 (t, *J* = 7.0 Hz, 2H), 2.27 (t, *J* = 7.5 Hz, 2H), 1.55 – 1.65 (m, 4H), 1.20 – 1.40 (m, 17H). ¹³C NMR (125 MHz, CDCl₃): δ 173.89, 60.15, 51.46, 34.34, 29.37, 29.35 (2C), 29.33, 29.23, 29.10, 28.79, 26.67, 24.92, 14.23. HRMS (ESI) *m/z* [M+H]⁺ calcd for C₁₄H₂₈N₃O₂, 269.2176; found, 269.2176.

Ethyl 15-azidopentadecanoate (9)

To a solution of triphenyl phosphine (2.633g, 10.04 mmol) in anhydrous tetrahydrofuran (THF; 40 mL) at 0°C was added diisopropyl azodicarboxylate (2.029g, 10.04 mmol) dropwise. The mixture was stirred for 10 min, and then alcohol **5** (2.388g, 8.36 mmol) in THF (20 mL) was added dropwise. After 30 min diphenyl phosphoryl azide (2.763g, 10.04 mmol) was added and the mixture was warmed to room temperature and stirred for 4.5 h. Water (80 mL), diethyl ether (150 mL) and brine (100 mL) was then added, and the ether layer was separated and concentrated under reduced pressure. The residue was purified on silica gel by stepwise gradient elution with dichloromethane/hexane (20:80 to 100:0), yielding 1.516g (49%) of **9** as a pale yellow oil. ¹H NMR (500 MHz, CDCl₃): δ 4.10 (q, *J* = 7.0 Hz, 2H), 3.23 (t, *J* = 7.0 Hz, 2H), 2.26 (t, *J* = 7.5 Hz, 2H), 1.55 – 1.65 (m, 4H), 1.20 – 1.40 (m, 23H). ¹³C NMR (125 MHz, CDCl₃): δ 173.92, 60.13, 51.47, 34.37, 29.57 (2C), 29.55, 29.50, 29.44, 29.42, 29.24, 29.12 (2C), 28.81, 26.67, 24.96, 14.23. HRMS (ESI) *m/z* [M+H]⁺ calcd for C₁₂H₂₄N₃O₂, 312.2646; found, 312.2645.

General procedure for synthesis of amines

Azides **6 - 9** (4.81 mmol) and triphenyl phosphine (6.25 mmol) were dissolved in anhydrous THF (30 mL) and stirred at room temperature for 8 h. Water (9.62 mmol) was then added, and the reaction was stirred for 16 h. The reaction was concentrated under reduced pressure and the residue was purified on silica gel by stepwise gradient elution with dichloromethane/methanol (95:5 to 40:60), yielding the desired products as solids.

Ethyl 10-aminodecanoate (10). White solid, 71% yield. ¹H NMR (400 MHz, CDCl₃): δ 4.10 (q, *J* = 7.2 Hz, 2H), 2.65 (t, *J* = 7.2 Hz, 2H), 2.26 (t, *J* = 7.6 Hz, 2H), 1.59 (p, *J* = 7.2 Hz, 2H), 1.41 (p, *J* = 7.2 Hz, 2H), 1.20 – 1.35 (m, 13H). ¹³C NMR (100 MHz, CDCl₃): δ 173.90, 60.13, 42.17, 34.35, 33.73, 29.38 (2C), 29.17, 29.08, 26.81, 24.93, 14.22. HRMS (ESI) *m/z* [M+H]⁺ calcd for C₁₂H₂₆NO₂, 216.1958; found, 216.1955.

Ethyl 11-aminoundecanoate (11). White solid, 96% yield. ¹H NMR (400 MHz, CDCl₃): δ 4.10 (q, *J* = 7.2 Hz, 2H), 2.66 (t, *J* = 7.2 Hz, 2H), 2.26 (t, *J* = 7.6 Hz, 2H), 1.59 (p, *J* = 7.6 Hz, 2H), 1.41 (p, *J* = 6.8 Hz, 2H), 1.20 – 1.35 (m, 15H). ¹³C NMR (100 MHz, CDCl₃): δ 173.91, 60.13, 42.19, 34.36, 33.73, 29.51, 29.43, 29.35, 29.21, 29.10, 26.84, 24.94, 14.22. HRMS (ESI) *m/z* [M+H]⁺ calcd for C₁₃H₂₈NO₂, 230.2114; found, 230.2110.

Ethyl 12-aminododecanoate (12). White solid, 96% yield. ¹H NMR (400 MHz, CDCl₃): δ 4.10 (q, *J* = 7.2 Hz, 2H), 2.65 (t, *J* = 6.8 Hz, 2H), 2.26 (t, *J* = 7.6 Hz, 2H), 1.59 (p, *J* = 7.2 Hz, 2H), 1.41 (p, *J* = 6.8 Hz, 2H), 1.20 – 1.35 (m, 17H). ¹³C NMR (100 MHz, CDCl₃): δ 173.90, 60.11, 42.24, 34.35, 33.86, 29.55, 29.49, 29.46, 29.39, 29.21, 29.10, 26.86, 24.94, 14.22. HRMS (ESI) *m/z* [M+H]⁺ calcd for C₁₄H₃₀NO₂, 244.2271; found, 244.2271.

Ethyl 15-aminopentadecanoate (13). White solid, 86% yield. ¹H NMR (400 MHz, CDCl₃): δ 4.10 (q, *J* = 7.2 Hz, 2H), 2.66 (t, *J* = 7.2 Hz, 2H), 2.26 (t, *J* = 7.6 Hz, 2H), 1.59 (p, *J* = 7.2 Hz, 2H), 1.39 (p, *J* = 7.2 Hz, 2H), 1.20 – 1.35 (m, 23H). ¹³C NMR (100 MHz, CDCl₃): δ 173.89, 60.11, 42.19, 34.37, 33.73, 29.60 (2C), 29.59, 29.58, 29.55, 29.47, 29.42, 29.23, 29.11, 26.86, 24.96, 14.22. HRMS (ESI) *m/z* [M+H]⁺ calcd for C₁₇H₃₆NO₂, 286.2741; found, 286.2736.

General procedure for synthesis of ureas from amines

To a solution of the amine (**10-13**, 1.50 mmol) in anhydrous THF (15 mL) under a nitrogen atmosphere was added 4-chloro-3-(trifluoromethyl)phenyl isocyanate (1.65 mmol). The mixture was stirred at room temperature for 2 h, and then concentrated under reduced pressure. The residue was purified on silica gel by stepwise gradient elution with dichloromethane/ethyl acetate (100:0 to 80:20), yielding the products as solids.

Ethyl 10-((4-chloro-3-(trifluoromethyl)phenyl)carbamoyl)amino)decanoate (17a). White solid, 82% yield. ¹H NMR (500 MHz, CDCl₃): δ 7.55-7.65 (m, 2H), 7.53 (dd, *J* = 9.0, 2.5 Hz, 1H), 7.33 (d, *J* = 9.0 Hz, 1H), 5.40 (s, 1H), 4.13 (q, *J* = 7.0 Hz, 2H), 3.20 (t, *J* = 7.0 Hz, 2H), 2.30 (t, *J* = 7.0 Hz, 2H), 1.59 (p, *J* = 7.0 Hz, 2H), 1.44 (p, *J* = 7.0 Hz, 2H), 1.35 – 1.18 (m, 13H). ¹³C NMR (125 MHz, CDCl₃): δ 174.68, 155.56, 138.25, 131.84, 128.53 (q, *J* = 31 Hz), 124.85, 122.85, 122.64 (q, *J* = 272 Hz), 117.81 (q, *J* = 6 Hz), 60.48, 40.16, 34.34, 29.79, 29.01, 28.89, 28.83, 28.81, 26.60, 24.83, 14.18. HRMS (ESI) *m/z* [M+H]⁺ calcd for C₂₀H₄₁ClF₃N₂O₃, 437.1813; found, 437.1813.

Ethyl 11-((4-chloro-3-(trifluoromethyl)phenyl)carbamoyl)amino)undecanoate (17b). White solid, 62% yield. ¹H NMR (500 MHz, CDCl₃): δ 7.61 (d, *J* = 2.5 Hz, 1H), 7.55 (dd, *J* = 9.0, 2.5 Hz, 1H), 7.38-7.34 (m, 2H), 5.22 (t, *J* = 5.5 Hz, 1H), 4.13 (q, *J* = 7.0 Hz, 2H), 3.22 (q, *J* = 6.5 Hz, 2H), 2.30 (t, *J* = 7.5 Hz, 2H), 1.61 (p, *J* = 7.5 Hz, 2H), 1.44 (p, *J* = 7.5 Hz, 2H), 1.35-1.20 (m, 15H). ¹³C NMR (125 MHz, CDCl₃): δ 174.64, 155.31, 138.21, 131.87, 128.57 (q, *J* = 31 Hz), 124.94, 122.91, 122.60 (q, *J* = 272 Hz), 117.88 (q, *J* = 6 Hz), 60.45, 40.26, 34.40, 29.86, 29.16, 29.00, 28.92, 28.89, 28.87, 26.66, 24.82, 14.10. HRMS (ESI) *m/z* [M+H]⁺ calcd for C₂₂H₄₃ClF₃N₂O₃, 451.1970; found, 451.1969.

Ethyl 12-((4-chloro-3-(trifluoromethyl)phenyl)carbamoyl)amino)dodecanoate (17c). White solid, 56% yield. ¹H NMR (500 MHz, CDCl₃): δ 7.60 (d, *J* = 2.5 Hz, 1H), 7.54 (dd, *J* = 9.0, 2.5 Hz, 1H), 7.38 (s, 1H), 7.34 (d, *J* = 9.0 Hz, 1H), 5.26 (t, *J* = 5.5 Hz, 1H), 4.13 (q, *J* = 7.5 Hz, 2H), 3.22 (q, *J* = 7.0 Hz, 2H), 2.30 (t, *J* = 7.0 Hz, 2H), 1.60 (p, *J* = 7.0 Hz, 2H), 1.47 (p, *J* = 7.0 Hz, 2H), 1.35 – 1.20 (m, 17H). ¹³C NMR (125 MHz, CDCl₃): δ 174.59, 155.37, 138.18, 131.86, 128.53 (q, *J* = 31 Hz), 124.96, 122.93, 122.60 (q, *J* = 272 Hz), 117.86 (q, *J* = 6 Hz), 60.42, 40.30, 34.42, 29.91, 29.28, 29.16, 29.12, 29.08, 29.03, 28.94, 26.74, 24.89, 14.19. HRMS (ESI) *m/z* [M+H]⁺ calcd for C₂₂H₄₅ClF₃N₂O₃, 465.2126; found, 465.2125.

Ethyl 15-({[4-chloro-3-(trifluoromethyl)phenyl]carbamoyl}amino)pentadecanoate (17f).

White solid, 80% yield. ¹H NMR (500 MHz, CDCl₃): δ 7.59 (d, *J* = 2.5 Hz, 1H), 7.52 (dd, *J* = 8.5, 2.5 Hz, 1H), 7.45 (s, 1H), 7.33 (d, *J* = 8.5 Hz, 1H), 5.35 (s, 1H), 4.13 (q, *J* = 7.0 Hz, 2H), 3.20 (t, *J* = 7.0 Hz, 2H), 2.30 (t, *J* = 7.5 Hz, 2H), 1.61 (p, *J* = 7.5 Hz, 2H), 1.47 (p, *J* = 7.0 Hz, 2H), 1.35 – 1.20 (m, 23H). ¹³C NMR (125 MHz, CDCl₃): δ 174.54, 155.48, 138.15, 131.84, 128.56 (q, *J* = 31 Hz), 124.98, 121.54, 122.60 (q, *J* = 272 Hz), 117.93 (q, *J* = 6 Hz), 60.39, 40.46, 34.46, 29.82, 29.42, 29.38 (4C), 29.28, 29.22, 29.13, 29.05, 26.83, 24.97, 14.19. HRMS (ESI) *m/z* [M+H]⁺ calcd for C₂₅H₅₁ClF₃N₂O₃, 507.2596; found, 507.2596.

General procedure for synthesis of ureas from cyano esters

To a solution of NiCl₂·6H₂O (1.87 mmol) and a cyano ester (**14-16**, 0.93 mmol) in methanol (20 mL) at 0°C was added NaBH₄ (0.361 g, 9.53 mmol) over 30 min. The black reaction mixture was allowed to warm to room temperature, and was then stirred for 1.5 h. 1M HCl was added until the black precipitate disappeared. The mixture was made alkaline with concentrated NH₄OH solution and extracted with dichloromethane (3 x 30 mL). The combined extracts were dried over Na₂SO₄ and concentrated under reduced pressure. The residue was then dissolved in anhydrous in anhydrous THF (15 mL) under a nitrogen atmosphere. 4-Chloro-3-(trifluoromethyl)phenyl isocyanate (0.066 g, 0.93 mmol) was added and the mixture was stirred at room temperature for 2 h, and then concentrated. The residue was purified on silica gel by stepwise gradient elution with dichloromethane/ethyl acetate (100:0 to 75:25), yielding the desired products as white solids.

Ethyl 13-({[4-chloro-3-(trifluoromethyl)phenyl]carbamoyl}amino)tridecanoate (17d).

White solid, 70% yield. ¹H NMR (500 MHz, CDCl₃): δ 7.60 (d, *J* = 2.5 Hz, 1H), 7.53 (dd, *J* = 8.5, 2.5 Hz, 1H), 7.41 (s, 1H), 7.33 (d, *J* = 8.5 Hz, 1H), 5.30 (t, *J* = 5.5 Hz, 1H), 4.13 (q, *J* = 7.0 Hz, 2H), 3.21 (t, *J* = 6.5 Hz, 2H), 2.31 (t, *J* = 7.5 Hz, 2H), 1.60 (p, *J* = 7.5 Hz, 2H), 1.47 (p, *J* = 7.5 Hz, 2H), 1.35 – 1.18 (m, 19H). ¹³C NMR (125 MHz, CDCl₃): δ 174.59, 155.41, 138.18, 131.85, 128.54 (q, *J* = 31 Hz), 124.94, 122.93, 122.61 (q, *J* = 273 Hz), 117.88 (q, *J* = 6 Hz), 60.41, 40.31, 34.43, 29.92, 29.28, 29.27, 29.24, 29.13, 29.12, 29.05, 28.99, 26.75, 24.90, 14.19. HRMS (ESI) *m/z* [M+H]⁺ calcd for C₂₃H₄₇ClF₃N₂O₃, 479.2283; found, 479.2285.

Ethyl 14-({[4-chloro-3-(trifluoromethyl)phenyl]carbamoyl}amino)tetradecanoate (17e).

White solid, 64% yield. ¹H NMR (500 MHz, CDCl₃): δ 7.60 (d, *J* = 2.5 Hz, 1H), 7.55 (dd, *J* = 8.5, 2.5 Hz, 1H), 7.34 (d, *J* = 8.5 Hz, 1H), 7.23 (s, 1H), 5.17 (t, *J* = 5.5 Hz, 1H), 4.13 (q, *J* = 7.0 Hz, 2H), 3.21 (q, *J* = 6.0 Hz, 2H), 2.29 (t, *J* = 7.5 Hz, 2H), 1.59 (p, *J* = 7.5 Hz, 2H), 1.44 (p, *J* = 7.5 Hz, 2H), 1.35 – 1.18 (m, 21H). ¹³C NMR (125 MHz, CDCl₃): δ 174.50, 155.25, 138.14, 131.86, 128.57 (q, *J* = 31 Hz), 125.02, 122.98, 122.57 (q, *J* = 273 Hz), 117.91 (q, *J* = 6 Hz), 60.37, 40.37, 34.75, 29.96, 29.36, 29.34, 29.31, 29.30, 29.21, 29.17, 29.12, 29.02, 26.78, 24.93, 14.20. HRMS (ESI) *m/z* [M+H]⁺ calcd for C₂₄H₄₉ClF₃N₂O₃, 493.2439; found, 493.2437.

Ethyl 17-({[4-chloro-3-(trifluoromethyl)phenyl]carbamoyl}amino)heptadecanoate (17h).

White solid, 58% yield. ¹H NMR (500 MHz, CDCl₃): δ 7.60 (d, *J* = 2.5 Hz, 1H), 7.55 (dd, *J* = 8.5, 2.5 Hz, 1H), 7.35 (d, *J* = 9.0 Hz, 1H), 7.11 (s, 1H), 5.10 (t, *J* = 5.5 Hz, 1H), 4.13 (q, *J* = 7.0 Hz, 2H), 3.21 (q, *J* = 6.5 Hz, 2H), 2.30 (t, *J* = 7.5 Hz, 2H), 1.60 (p, *J* = 7.5 Hz, 2H), 1.48 (p, *J* = 7.5 Hz, 2H), 1.35 – 1.18 (m, 27H). ¹³C NMR (125 MHz, CDCl₃): δ 174.44, 155.14, 138.09, 131.88, 128.51 (q, *J* = 32 Hz), 125.06, 123.03, 122.42 (q, *J* = 272 Hz), 117.98 (q, *J* = 6 Hz), 60.35, 40.42, 34.46, 30.02, 29.43, 29.41 (6C), 29.32, 29.24, 29.18, 29.09, 26.85, 24.99, 14.20. HRMS (ESI) *m/z* [M+H]⁺ calcd for C₂₇H₅₅ClF₃N₂O₃, 535.2909; found, 535.2909.

General procedure for ester hydrolysis

The ester (**17a - 17h**, 0.80 mmol) was dissolved in ethanol (30 mL) at 40°C, and 1.5M NaOH (10 mL) was added dropwise. The reaction was stirred for 4 h. The volume of the reaction solvent was reduced by half under reduced pressure, and then acidified with 1M HCl to a pH of 1-2. The resulting precipitate was then filtered and washed with H₂O, followed by H₂O/ethanol (1:1), and dried on a Buchner funnel.

10-({[4-chloro-3-(trifluoromethyl)phenyl]carbamoyl}amino)decanoic acid (1a).

White solid, 78% yield. Mp = 110 – 111°C. ¹H NMR (500 MHz, DMSO-*d*₆): δ 11.93 (s, 1H), 8.88 (s, 1H), 8.04 (d, *J* = 2.0 Hz, 1H), 7.45-7.55 (m, 2H), 6.28 (t, *J* = 5.5 Hz, 1H), 3.05 (q, *J* = 7.0 Hz, 2H), 2.16 (t, *J* = 7.0 Hz, 2H), 1.35-1.50 (m, 4H), 1.20-1.30 (m, 10H). ¹³C NMR (125 MHz, DMSO-*d*₆): δ 174.93, 155.29, 140.68, 132.25, 126.96 (q, *J* = 31 Hz), 123.33 (q, *J* = 271 Hz), 122.66, 121.61, 116.45 (q, *J* = 6 Hz), 34.10, 30.04, 29.47, 29.34, 29.16, 29.15, 28.98, 26.77, 24.93. HRMS (ESI) *m/z* [M+H]⁺ calcd for C₁₈H₂₄ClF₃N₂O₃, 409.1500; found, 409.1501.

11-({[4-chloro-3-(trifluoromethyl)phenyl]carbamoyl}amino)undecanoic acid (1b).

White solid, 63% yield. Mp = 113 – 114°C. ¹H NMR (500 MHz, DMSO-*d*₆): δ 11.93 (s, 1H), 8.90 (s, 1H), 8.04 (d, *J* = 2.0 Hz, 1H), 7.45-7.55 (m, 2H), 6.30 (t, *J* = 5.5 Hz, 1H), 3.06 (q, *J* = 7.0 Hz, 2H), 2.16 (t, *J* = 7.0 Hz, 2H), 1.35-1.50 (m, 4H), 1.20-1.30 (m, 12H). ¹³C NMR (125 MHz, DMSO-*d*₆): δ 174.95, 155.29, 140.68, 132.23, 126.95 (q, *J* = 31 Hz), 123.33 (q, *J* = 271 Hz), 122.64, 121.62, 116.47 (q, *J* = 6 Hz), 34.18, 30.04, 29.42, 29.31, 29.18, 29.00, 26.78, 24.94. HRMS (ESI) *m/z* [M+H]⁺ calcd for C₁₉H₂₆ClF₃N₂O₃, 423.1657; found, 423.1657.

12-({[4-chloro-3-(trifluoromethyl)phenyl]carbamoyl}amino)dodecanoic acid (1c).

White solid, 72% yield. Mp = 131 – 132°C. ¹H NMR (500 MHz, DMSO-*d*₆): δ 11.95 (s, 1H), 9.11 (s, 1H), 8.05 (d, *J* = 2.0 Hz, 1H), 7.50-7.65 (m, 2H), 6.49 (t, *J* = 5.5 Hz, 1H), 3.04 (q, *J* = 7.0 Hz, 2H), 2.13 (t, *J* = 7.0 Hz, 2H), 1.50-1.60 (m, 4H), 1.15-1.25 (m, 14H). ¹³C NMR (125 MHz, DMSO-*d*₆): δ 175.18, 155.39, 140.82, 132.21, 127.27 (q, *J* = 31 Hz), 123.34 (q, *J* = 271 Hz), 122.62, 121.50, 116.43 (q, *J* = 6 Hz), 34.39, 30.00, 29.37, 29.26, 29.24, 29.15, 29.13, 28.96, 26.74, 25.00. HRMS (ESI) *m/z* [M+H]⁺ calcd for C₂₀H₂₈ClF₃N₂O₃, 437.1813; found, 437.1814.

13-({[4-chloro-3-(trifluoromethyl)phenyl]carbamoyl}amino)tridecanoic acid (1d).

White solid, 59% yield. Mp = 135 – 136°C. ¹H NMR (500 MHz, DMSO-*d*₆): δ 10.75 (s, 1H), 8.13 (d, *J* = 2.5 Hz, 1H), 7.96 (s, 1H), 7.61 (dd, *J* = 2.5, 9.0 Hz, 1H), 7.45 (d, *J* = 9.0 Hz, 1H), 3.01 (q, *J* = 7.0 Hz, 2H), 2.01 (t, *J* = 7.0 Hz, 2H), 1.44 (q, *J* = 7.0 Hz, 2H), 1.36 (q, *J* = 7.0 Hz, 2H), 1.15-1.25 (m, 16H). ¹³C NMR (125 MHz, DMSO-*d*₆): δ 177.11, 156.06, 141.77, 131.96, 126.71 (q, *J* = 31 Hz), 123.33 (q, *J* = 272 Hz), 122.02, 120.59, 116.16 (q, *J* = 6 Hz), 30.05, 29.25, 29.14, 29.02, 28.99 (2C), 28.95, 28.85, 26.70, 26.01. HRMS (ESI) *m/z* [M+H]⁺ calcd for C₂₁H₃₀ClF₃N₂O₃, 451.1970; found, 451.1969.

14-({[4-chloro-3-(trifluoromethyl)phenyl]carbamoyl}amino)tetradecanoic acid (1e).

White solid, 64% yield. Mp = 100 – 102°C. ¹H NMR (500 MHz, DMSO-*d*₆): δ 8.93 (s, 1H), 8.06 (d, *J* = 2.5 Hz, 1H), 7.50-7.60 (m, 2H), 6.33 (t, *J* = 5.5 Hz, 1H), 3.07 (q, *J* = 6.5 Hz, 2H), 2.17 (t, *J* = 7.0 Hz, 2H), 1.35-1.50 (m, 4H), 1.20-1.30 (m, 18H). ¹³C NMR (125 MHz, DMSO-*d*₆): δ 174.53, 154.85, 140.25, 131.79, 126.54 (q, *J* = 31 Hz), 122.88 (q, *J* = 271 Hz), 122.20, 121.15, 116.04, 33.96, 29.57, 29.00 (2C), 28.97 (2C), 28.89, 28.73 (2C), 28.53, 26.30, 24.50. HRMS (ESI) *m/z* [M+H]⁺ calcd for C₂₂H₃₂ClF₃N₂O₃, 465.2126; found, 465.2127.

15-([4-chloro-3-

(trifluoromethyl)phenyl]carbamoyl)amino)pentadecanoic acid (1f). White solid, 93% yield. Mp = 97-98 °C. ¹H NMR (500 MHz, DMSO-d₆): δ 11.93 (s, 1H), 8.90 (s, 1H), 8.04 (d, *J* = 2.5 Hz, 1H), 7.45-7.55 (m, 2H), 6.30 (t, *J* = 6.0 Hz, 1H), 3.05 (q, *J* = 6.5 Hz, 2H), 2.16 (t, *J* = 7.5 Hz, 2H), 1.35-1.50 (m, 4H), 1.20-1.30 (m, 20H). ¹³C NMR (125 MHz, DMSO-d₆): δ 174.97, 155.30, 140.70, 132.24, 126.96 (q, *J* = 30 Hz), 123.32 (q, *J* = 271 Hz), 122.65, 121.61, 116.47 (q, *J* = 6 Hz), 34.14, 30.21, 29.74 (2C), 29.45, 29.43, 29.42, 29.35, 29.18 (2C), 28.99, 29.75, 24.95. HRMS (ESI) *m/z* [M+H]⁺ calcd for C₂₃H₃₄ClF₃N₂O₃, 479.2283; found, 479.2284.

17-([4-chloro-3-

(trifluoromethyl)phenyl]carbamoyl)amino)heptadecanoic acid (1h). White solid, 82% yield. Mp = 79-80 °C. ¹H NMR (500 MHz, DMSO-d₆): δ 11.94 (s, 1H), 8.94 (s, 1H), 8.04 (d, *J* = 2.5 Hz, 1H), 7.50-7.60 (m, 2H), 6.33 (t, *J* = 5.5 Hz, 1H), 3.05 (q, *J* = 6.5 Hz, 2H), 2.15 (t, *J* = 7.0 Hz, 2H), 1.35-1.50 (m, 4H), 1.15-1.30 (m, 10H). ¹³C NMR (125 MHz, DMSO-d₆): δ 174.99, 155.31, 140.72, 132.24, 126.94 (q, *J* = 31 Hz), 123.32 (q, *J* = 270 Hz), 122.65, 121.59, 116.49, 34.18, 30.02, 29.46 (4C), 29.43, 29.41, 29.40, 29.33, 29.18, 29.16, 28.99, 26.74, 24.96. HRMS (ESI) *m/z* [M+H]⁺ calcd for C₂₅H₃₈ClF₃N₂O₃, 507.2596; found, 507.2597.

Cell based assays

Biochemicals: Dulbecco's Modified Eagle's Medium (DMEM), Fetal Bovine Serum (FBS), trypsin/EDTA, penicillin and streptomycin, phosphate-buffered saline (PBS) and biochemicals were obtained from Sigma-Aldrich Chemical (Castle Hill, NSW, Australia). JC-1 was from Cayman Chemical (Ann Arbor, MI, USA).

Cell culture and viability assays: Human MDA-MB-231 breast cancer cells were obtained from ATCC (Manassas, VA, USA) and grown at 37°C in a humidified atmosphere of 5% CO₂ in air in DMEM that was supplemented with 10% FBS and 1% penicillin/streptomycin. The control MCF10A cell line was a gift from Prof Christine Clarke (Westmead Institute for Medical Research, Westmead, NSW, Australia). Confluent cells (80-90%) were harvested using Trypsin/EDTA after washing with PBS. Cells were treated with various concentrations of **1g** analogues in DMSO (final concentration 0.1%); control cells were treated with DMSO alone. ATP formation was assessed using the CellTiter-Glo® assay (Promega; Annandale, NSW, Australia) as described previously.^[13]

Cell cycle kinetics: MDA-MB-231 cells were seeded at a density of 7 x 10⁴ cells/well in 12-well plates and allowed to adhere overnight. After serum starvation for 24 h, the cells were treated with test compounds (10 μM) in DMSO for 48 h; control cells received serum-free DMEM alone. Cells were trypsinized, washed with PBS and fixed overnight with cold ethanol (80%, -20°C). The cells were washed twice with PBS and resuspended in 0.1M PBS containing 0.1 mg/mL DNase-free RNase A and 0.1% NP40. The cells were incubated on ice for 1 h with propidium iodide and analysed as described previously in a Gallios flow cytometer (Beckman Coulter Australia, Lane Cove, NSW).^[20]

Annexin V-FITC/7AAD: Annexin V-FITC/7AAD staining in treated MDA-MB 231 cells (7 x 10⁴ cells/well) was assessed in 12-well plates. Twenty four h after serum removal the cells were treated with compounds (10 μM) for 24 or 48 h. Treated cells were trypsinized and washed twice with cold PBS and then stained with annexin V-FITC and 7AAD for analysis in a Gallios™ flow cytometer (Beckman Coulter Australia).^[20]

JC-1 assay: MDA-MB-231 cells were seeded in triplicate in 96-well plates (1x10⁴ cells/well) and 24 h later serum was removed. Cells were treated with various concentrations of the test compounds for 1 h; control cells received serum-free DMEM. Cells were incubated with JC-1 in serum-free medium (37°C, 20 min) and the JC-1 red:green ratio was estimated (JC-1 Mitochondrial Membrane Potential Assay Kit; Cayman Chemical, Ann Arbor, MI).

Fluorescence microscopy: MDA-MB-231 cells were seeded in 12-well plates and cultured for 24 h in DMEM medium supplemented with 10% FBS and 1% penicillin/streptomycin. After serum deprivation for 16 h, cells were treated with **1g** analogues (10 μM, 4 h) or DMSO in serum-free DMEM. Following two washes with serum-free medium, cells were incubated with JC-1 and Hoechst 33258 (Sigma-Aldrich) for 20 min, according to the manufacturer's instructions. Images of JC-1 aggregates (red), JC-1 monomers (green) and nuclear staining (blue) of cells were acquired with a fluorescence microscope (Olympus BX51, Notting Hill, VIC, Australia).

Statistical analysis: All data are expressed throughout as means ± SEM. Data were analyzed by one-way ANOVA and the Fisher's Partial Least-Squares Difference test was used to detect differences between multiple treatments. All experiments were replicated on 3-4 occasions.

Acknowledgements

This study was supported by grants from the Australian National Health and Medical Research Council (1031686 and 1087248). We are grateful to Prof Christine Clarke of the Westmead Institute for Medical Research (Westmead, NSW, Australia) for the generous gift of MCF10A cells.

Contributor roles

Designed research (MM, TR), performed experiments (TR, AR, YC, KB), analysed data (MM, AR, YC, KB, TR), drafted manuscript (MM, TR)

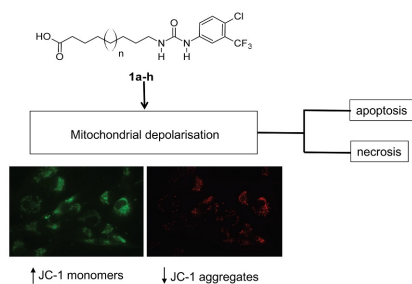
Keywords: antitumor agents, apoptosis, breast cancer, fatty acids, lipid drugs

References

- [1] S. Fulda, L. Galluzzi, G. Kroemer, *Nat Rev. Drug Discov.* **2010**, *9*, 447-464.
- [2] D.P. Rose, J.M. Connolly, *J. Natl Cancer Inst.* **1993**, *85*, 1743-1747.
- [3] W.E. Hardman, *J. Nutr.* **2002**, *132*, 3508S-3512S.
- [4] A.P. Simopoulos, *Biomed. Pharmacother.* **2002**, *56*, 365-379.
- [5] M. Murray, A. Hraiki, M. Bebaawy, C. Pazderka, T. Rawling, *Pharmacol. Ther.* **2015**, *150*, 109-128.
- [6] F.P. Guengerich, *Adv. Pharmacol.* **1997**, *43*, 7-35.
- [7] S.A. Wrighton, J.C. Stevens, *Crit. Rev. Toxicol.* **1992**, *22*, 1-21.
- [8] G.C. Farrell, M. Murray, *Gastroenterology* **1990**, *99*, 885-889.
- [9] M. Murray, E. Cantrill, R. Martini, G.C. Farrell, *Arch Biochem Biophys.* **1991**, *286*, 618-624.
- [10] X. Xu, X.A. Zhang, D.W. Wang, *Adv. Drug Deliv. Rev.* **2011**, *63*, 597-609.
- [11] P.H. Cui, N. Petrovic, M. Murray, *Br. J. Pharmacol.* **2011**, *162*, 1143-1155.
- [12] G.Zhang, D. Panigrahy, L.M. Mahakian, J. Yang, J.Y. Liu, K.S. Stephen Lee, H.I. Wettersten, A. Ulu, X. Hu, S. Tam, S.H. Hwang, E.S. Ingham, M.W. Kieran, R.H. Weiss, K.W. Ferrara, B.D. Hammock, *Proc. Natl Acad. Sci. U. S. A.* **2013**, *110*, 6530-6535.
- [13] H.R.E. Dyari, T. Rawling, K. Bourget, M. Murray, *J. Med. Chem.* **2014**, *57*, 7459-7464.
- [14] H.R.E. Dyari, T. Rawling, Y. Chen, W. Sudarmana, K. Bourget, J.M. Dwyer, S.E. Allison, M. Murray, *FASEB J.* **2017**, *31*, 5246-5257.
- [15] C. Morisseau, B.D. Hammock, *Annu. Rev. Pharmacol. Toxicol.* **2013**, *53*, 37-58.

- [16] J. R. Falck, G. Wallukat, N. Puli, M. Goli, C. Arnold, A. Konkel, M. Rothe, R. Fischer, D.N. Müller, W.H. Schunck, *J. Med. Chem.* **2011**, *54*, 4109-4118.
- [17] J. R. Falck, R. Kodela, R. Manne, K.R. Atcha, N. Puli, N. Dubasi, V.L. Manthathi, J.H. Capdevila, X.Y. Yi, D.H. Goldman, C. Morisseau, B.D. Hammock, W.B. Campbell, *J. Med. Chem.* **2009**, *52*, 5069-5075.
- [18] T. Rawling, H. Choucair, N. Koolaji, K. Bourget, S.E. Allison, Y.J. Chen, C.R. Dunstan, M. Murray, *J. Med. Chem.* **2017**, *60*, 8661-8666.
- [19] Y. Al-Zubaidi, C.W. Pazderka, N. Koolaji, M.K. Rahman, H. Choucair, B. Umashankar, K. Bourget, Y. Chen, T. Rawling, M. Murray, *Eur. J. Pharm. Sci.* **2019**, *129*, 87-98.
- [20] N. Koolaji, T. Rawling, K. Bourget, M. Murray, *ChemMedChem*. **2018**, *13*, 1038-1043.
- [21] P.H. Cui, T. Rawling, K. Bourget, T. Kim, C.C. Duke, M.R. Doddareddy, D.E. Hibbs, F. Zhou, B.N. Tattam, N. Petrovic, M. Murray, *J. Med. Chem.* **2012**, *55*, 7163-7172.
- [22] T. Rawling, P.H. Cui, C.C. Duke, M. Murray. *Lipids* **2010**, *45*, 159-165.
- [23] M.G. Vander Heiden, L.C. Cantley, C.B. Thompson, *Science* **2009**, *324*[5930], 1029-1033.
- [24] B.G. Heerdt, M.A. Houston, A.H. Augenlicht, *Cell Growth Differ.* **1997**, *8*, 523-532.
- [25] M.E. Grossmann, N.K. Mizuno, M.L. Dammen, T. Schuster, A. Ray, M.P. Cleary. *Cancer Prev. Res.* **2009**, *2*, 879-886.
- [26] E.C. Yiannakopoulou, *Eur. J. Cancer Prevent.* **2015**, *24*, 416-421.
- [27] D.J. Ahnen, *Eur. J. Surg. Suppl.* **1998**, 111-114.
- [29] J.K. Fauser, L.D. Prisciandaro, A.G. Cummins, G.S. Howarth, *Cancer Biol. Ther.* **2011**, *11*, 724-731.
- [30] Y. Eguchi, S. Shimizu, Y. Tsujimoto, *Cancer Res.* **1997**, *57*, 1835-1840.
- [31] A. Koceva-Chyla, M. Jedrzejczak, J. Skierski, K. Kania, Z. Jozwiak, *Apoptosis* **2005**, *10*, 1497-1514.
- [32] A. Troyano, C. Fernandez, P. Sancho, E. de Blas, P. Aller, *J. Biol. Chem.* **2001**, *276*, 47107-47115.
- [33] S. Shen, O. Kepp, M. Michaud, I. Martins, H. Minoux, D. Metivier, M.C. Maiuri, R.T. Kroemer, G. Kroemer, *Oncogene* **2011**, *30*, 4544-4556.
- [34] S.N. Mostyn, J.E. Carland, S. Shimmon, R.M. Ryan, T. Rawling, R.J. Vandenberg, *ACS Chem Neurosci* **2017**, *8*, 1949-1959.

Entry for the Table of Contents



Alkyl chain was varied in the novel anti-cancer aryl-urea fatty acid **1g** (16-([4-chloro-3-(trifluoromethyl)phenyl]carbamoyl)amino)hexadecanoic acid). The C12-C17 analogues efficiently impaired the mitochondrial membrane potential and ATP production while shorter analogues were less active. **1g** and the C17 analogue also preferentially activated necrosis and apoptosis, respectively. Thus, alkyl chain length is a determinant of mitochondrial targeting by these agents and can be varied to develop analogues that activate apoptosis or necrosis in a regulated fashion.